Environmental and Ecological Statistics **7,** 239–254, 2000

Modeling and risk assessment for soil temperatures beneath prescribed forest fires

HAIGANOUSH K. PREISLER, SALLY M. HAASE and STEPHEN S. SACKETT

USDA Forest Service, Pacific Southwest Research Station, Riverside, CA

Received March 1998; Revised March 1999

Prescribed fire is a management tool used by wildland resource management organizations in many ecosystems to reduce hazardous fuels and to achieve a host of other objectives. To study the effects of fire in naturally accumulating fuel conditions, the ambient soil temperature is monitored beneath prescribed burns. In this study we developed a stochastic model for temperature profiles (values at 15 minute intervals) recorded at four depths beneath the soil during a large prescribed burn study. The model was used to assess the temporal fit of the data to particular solutions of the heat equation. We used a random effects model to assess the effects of observed site characteristics on maximum temperatures and to estimate risks of temperatures exceeding critical levels in future similar prescribed fires. Contour plots of estimated risks of temperatures exceeding 60°C for a range of fuel levels and soil depths indicated high risks of occurrence, especially when the moisture levels are low. However, the natural variability among sites seems to be large, even after controlling fuel and moisture levels, resulting in large standard errors of predicted risks.

Keywords: ambient temperature, autoregressive models, functional data, heat equation, nonlinear regression, random effects

1. Introduction

Selective, controlled burns known as prescribed fires are used by the USDA Forest Service and other land management organizations to achieve a variety of management objectives. Reducing surface fuels, thinning forest trees, releasing of seeds, and influencing insect and disease populations are important factors for the perpetuation of tree species. Together with the beneficial effects of prescribed fires come other more subtle effects that are of concern to wildland managers and the public at large. High soil temperatures beneath a prescribed burn can alter soil properties and may kill tree roots, seeds, and other soil biota essential to the ecosystem (Hungerford *et al*., 1991; Covington and Sackett, 1990). It is important to study soil temperatures around trees immediately after prescribed fires in order to determine soil and fuel conditions that might maximize the benefits of prescribed fire to the ecosystem, and at the same time minimize damage.

A large prescribed fire research study was started in 1988 in Sequoia and Kings Canyon National Parks, California to investigate the effects of fire in natural fuel conditions and to determine the extent of heating in the soil around individual trees (Haase and Sackett, 1998). Measurements were made using a thermocouple system devised by two of the authors (Sackett and Haase, 1992) specifically to monitor ambient soil temperatures beneath prescribed burns. Some questions of interest to scientists and forest managers are: (1) What are the effects of variables such as soil moisture, estimated fuel loadings, or different conifer ecosystems on soil temperature profiles (graphs of temperatures over time)? (2) What does an average temperature profile look like at a given soil depth? Scientists are interested in the risk of temperatures exceeding critical levels. For example, increases in mortality rates have been observed in many forms of soil organisms at temperatures between 34° and 40°C (Christiansen, 1964 and references within); plant tissue cannot survive temperatures greater than 45–65°C (Lorenz, 1939; Nelson, 1952; Kayll, 1963). (3) What are the estimated probabilities of soil temperatures exceeding these critical levels? This paper is concerned with obtaining answers to the above questions using the time/temperature profile data collected by two of the authors (S. Sackett and S. Haase) during seven prescribed fires over a period of 8 years.

Temperature profile data are ‘‘functional data’’. Each data point or record is a series of values of an underlying smooth function observed at discrete times (Ramsay and Silverman, 1997). In Section 2 we give methods for calculating summary statistics of functional data. The formulas are then used to produce average temperature profiles. In Section 3 we present a conceptual parametric model for heat profiles based on the differential equation for heat conduction. We use data from the prescribed fires to assess the goodness of fit of the conceptual model to soil temperature profiles. Focus of studies concerned with soil temperatures during prescribed fires have by and large been centered on developing computer simulation models designed to predict soil temperatures under forest and range fires (Campbell *et al*., 1995; Pafford *et al*., 1985; El-Doma *et al*., 1984). The purpose in developing a conceptual model in this study was to have a functional form that can then be used to convert discrete time data values to a continuous function. Such a function with a few physically meaningful parameters is useful for further analyses such as calculation of maxima from irregularly spaced records, estimation of durations of time with temperatures above critical levels, and estimation of measures of variability among records. Additionally, a stochastic model can be used to assess the suitability of specific conceptual-predictive models.

In Section 4 we study the effects of site characteristics, such as the amounts of fuel and amounts of soil moisture, on estimated maximum temperatures and construct 95% confidence intervals for the probability of soil temperatures in future fires, with similar characteristics, exceeding a critical level.

2. The data and some summary statistics

The data in this study are from seven prescribed fires conducted during summers and falls in the years between 1988–1995. In each fire, measurements were recorded at two or three locations around one giant sequoia and one sugar pine tree. Each site (tree) was used in only one fire. Temperature probes inserted at each location recorded temperatures at

approximately 15 minute intervals and for various depths. Data studied in this paper are from depths of 10, 20, 30, and 46 cm.

Fig. 1 provides graphs of the temperature profiles from all sites that included recordings at 10, 20, 30, or 46 cm beneath the soil surface. A fair amount of variability is seen among the curves in Fig. 1. Some of the curves with high temperatures are possibly from sites with high fuel loadings or low soil moisture levels. However, there seems to be a fair amount of variability not explained by any of the observed site characteristics. The temperature profiles in Fig. 2 are from two locations within the same fire with almost identical fuel loadings and moisture levels.

Some of the standard summary statistics, e.g., average and standard deviation, used in univariate data can also be useful for functional data. If $y_j(t_i)(i = 1, \ldots, I_j)$ denotes the measured temperature profile for a given depth at sites $j(j = 1, \ldots, N)$ and times $t_1, \ldots, t_{Ij}$ then an estimate of the mean profile over all sites is the function with values

$$\bar{y}(t_i) = \frac{1}{N}\sum_{j=1}^{N} y_j(t_i).$$

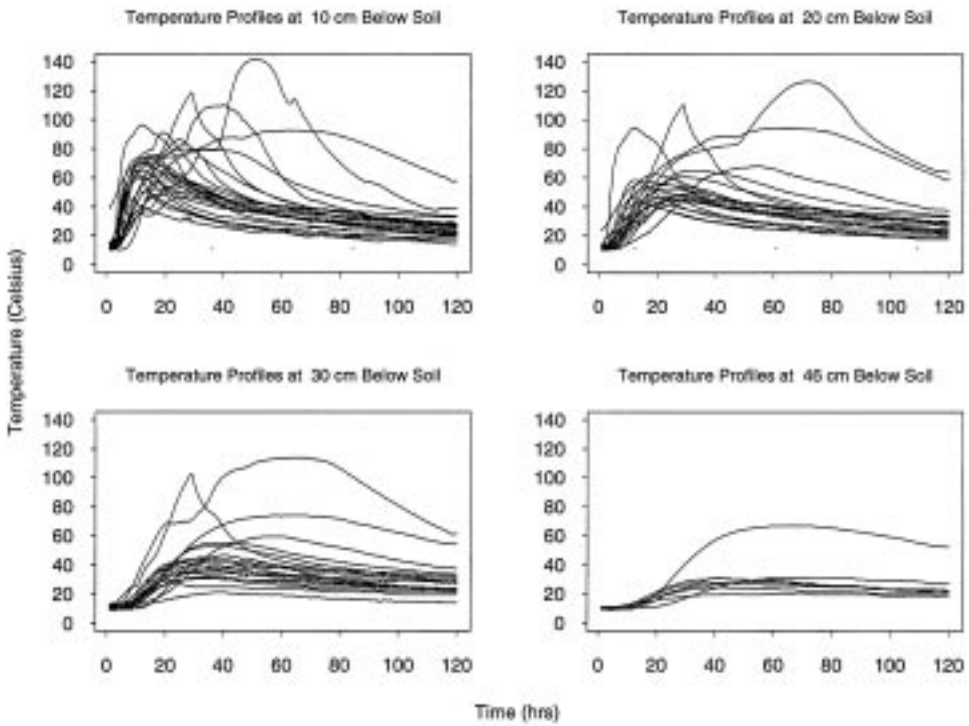

Figure 1. Profiles of temperatures beneath soil surface recorded during seven prescribed fires in Sequoia and Kings Canyon National Parks during summers and falls, 1988–1995. Before each fire, temperature probes were inserted at two or three locations around giant sequoia and sugar pine trees.

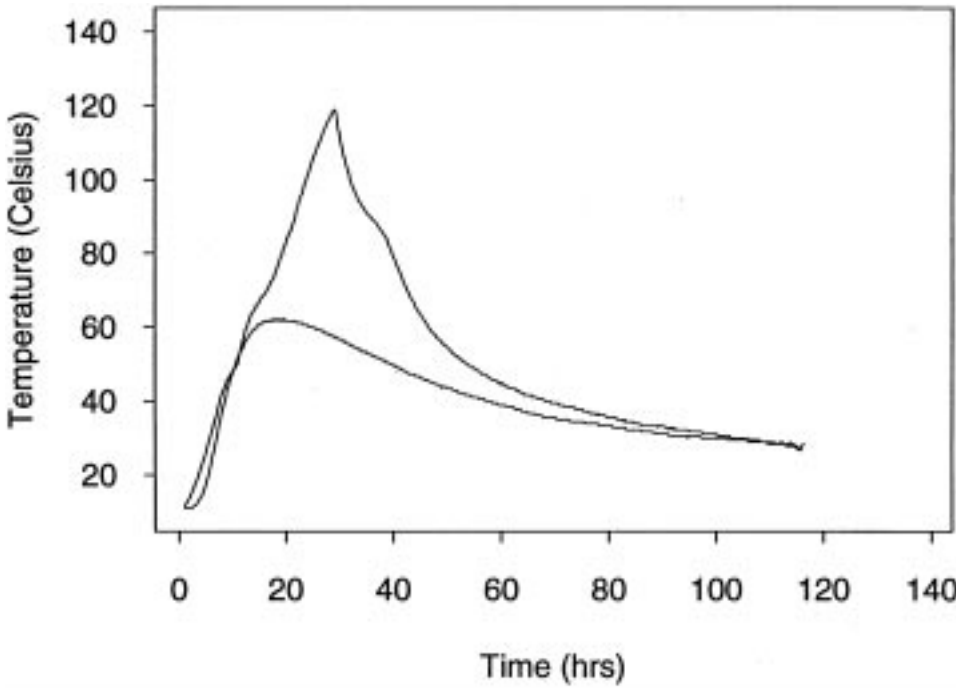

Figure 2. Two profiles of observed temperatures at 10 cm depth from two locations within the same fire with identical fuel loadings and moisture levels.

A typical sample of temperature profiles from prescribed burns often includes a small proportion of curves that are far removed from the rest. This was the case for the present sample (Fig. 1). A robust procedure for averaging curves is needed that is not overly influenced by one or two curves. Robust estimates for univariate data include the median and other trimmed means. Such estimates are also available for functional data (Brillinger, 1981; Folledo, 1983). The trimmed mean for functional data is calculated as follows. Given the distance measure

$$D_j(\mu) = \sum_{i=1}^{I_j} [y_j(t_i) - \mu(t_i)]^2$$

of each profile from a mean function $\mu(t)$, the trimmed mean is given by

$$\hat{\mu}(t_i) = \frac{1}{(1-\alpha)N} \sum_{j \in S} y_j(t_i)$$

where the sum is over the set, S, of profiles with the $(1-\alpha) \times N$ smallest distances $D_j(\hat{\mu})$. The estimate $\hat{\mu}(t)$ is computed iteratively starting with some initial mean profile such as the standard average function, $\bar{y}(t_i)$. The iteration is stopped when there is no further discernible change in the mean function. The 50% trimmed mean ($\alpha = 0.5$) is the median

in elemetary statistics. We expect the sample trimmed mean to be a better estimate of the population mean profile than the untrimmed mean.

Another summary statistic is the standard deviation function given by the square root of

$$s^2(t_i) = \frac{1}{N-1}\sum_{j=1}^{N}[y_j(t_i) - \bar{y}(t_i)]^2. \tag{1}$$

The standard deviation of the mean function $\bar{y}(t_i)$ is then given by $\frac{s(t_i)}{\sqrt{N}}$, assuming the curves are independent. Because formula (1) cannot be easily extended to estimate standard errors of the median or trimmed mean, we used the jackknife procedure (Efron, 1982) to estimate the required standard errors. The jackknife procedure is as follows: Delete one of the profiles from the data set and calculate the trimmed mean using only $N-1$ profiles. Repeat this process by deleting a different profile each time. This process will produce N different estimates of the mean. Next calculate the pseudo-observations

$$\bar{y}_j = N\hat{\mu} + (N-1)\hat{\mu}_{(j)}$$

where $\hat{\mu}_{(j)}$ is the trimmed mean of the data with the jth profile removed. The jackknife estimate of the variance is next obtained by replacing $\bar{y}(t_i)$ in (1) by $\hat{\mu}(t_i)$ and $y_j(t_i)$ by the pseudo-values $\bar{y}_j(t_i)$. When the parameter being estimated is the simple average, then

$$N\hat{\mu} = \sum_{all\ k} y_k;\ \ (N-1)\hat{\mu}_{(j)} = \sum_{k\neq j} y_k;$$

and the pseudo-observations are

$$\bar{y}_j = \sum_{all\ k} y_k - \sum_{k\neq j} y_k = y_j.$$

Thus, for the average the pseudo-observations are the same as the original observations and, consequently, the jackknife estimate of the variance is the usual variance estimate of the average as given by (1).

Fig. 3 provides graphs of the trimmed geometric means (with $\alpha = 0.2$) and approximate 95% pointwise confidence bars for four depths. Geometric means were used because histograms of log temperatures were more nearly symmetric than the corresponding histograms in the original units. The curves in Fig. 3 appear to indicate some significant drops in mean temperatures for every 10 cm drop in depth for the first 10 h after flames from the fire pass over a site and glowing combustion begins. Differences in mean temperatures at the four depths, however, stop being significant around two days after the start of the fire. Even 120 h after the start of the fire, mean temperatures at all four depths are still about 11°C higher than corresponding temperatures before the fire.

3. The heat equation—a conceptual model

Let $H(x,t)$ be the temperature of the material at a depth x from the soil surface at a time t. The flow of heat through a one dimensional homogenous material is often modeled by the equation of heat conduction

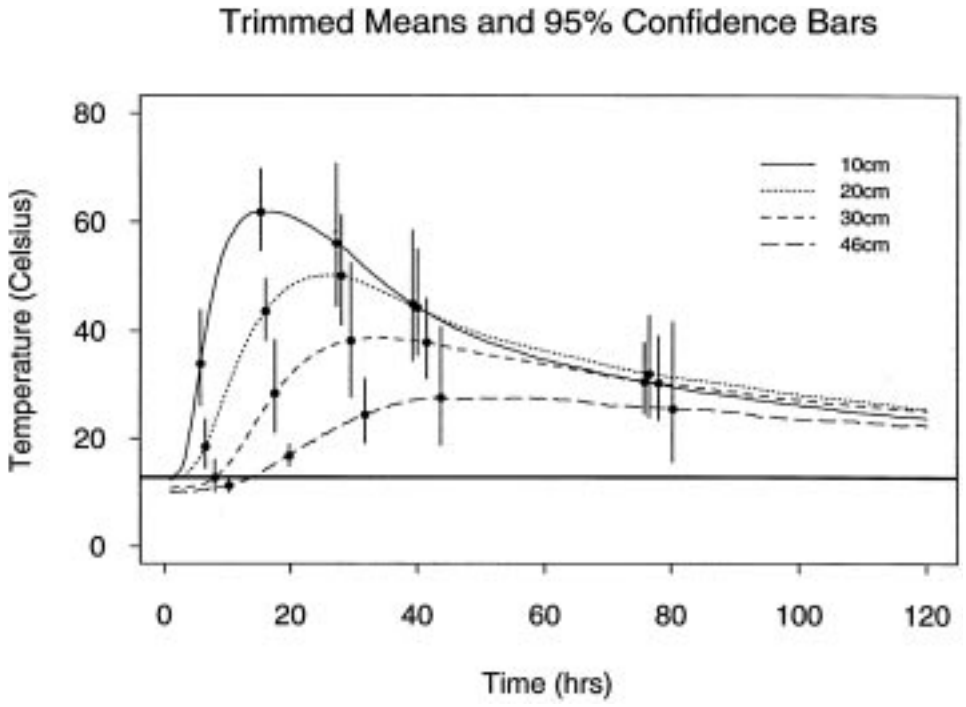

Figure 3. Trimmed geometric means and approximate 95% pointwise confidence bands (vertical bars). The horizontal bar at 11°C is the mean ambient soil temperature at 10 cm depth before the start of prescribed fire.

$$\frac{\partial H(x,t)}{\partial t} = \theta \frac{\partial^2 H(x,t)}{\partial x^2}. \tag{2}$$

The constant $\theta = k/c\rho$ is called the thermal diffusivity of the material and is assumed to depend on the conductivity (k), the specific heat (c), and the density (ρ) of the soil in the manner indicated (Widder, 1975). The above equation also assumes that there is no radiation of heat at the surface. We assume the initial and boundary conditions, $H(x,0) = C$ for $x>0$, $H(0,t) = b\delta(t)$ for $t>0$ where C is a constant and $\delta(t)$ the Dirac delta function. The boundary condition $H(x,0) = C$ specifies the background soil temperature before the start of the fire. Because variation in the background soil temperature is very small when compared with the magnitude of the temperatures during and after the fire, the assumption of constant background temperature is a reasonable approximation. For further convenience, we will assume C to be zero and remember to adjust the predicted temperatures accordingly. One solution to the partial differential Equation in (2) is the so-called derived source solution given by

$$H(x,t) = \frac{b}{(4\pi\theta)^{1/2}} x t^{-3/2} \exp\left(-\frac{x^2}{4\theta t}\right). \tag{3}$$

Equation (3) is called the source solution because it assumes that there is a source of heat of strength b at $x = 0$ (the soil surface).

If the surface is allowed to radiate heat at a fixed rate $\lambda(\geq 0)$ then the heat function can be derived as the solution of the differential equation

$$\frac{\partial H(x,t)}{\partial t} = \theta \frac{\partial^2 H(x,t)}{\partial x^2} - \lambda H(x,t) \tag{4}$$

(Piaggio, 1937). By putting $H(x,t) = e^{-\lambda} tG(x,t)$, Equation (4) is transformed to Equation (2) with $H(x,t)$ replaced by $G(x,t)$. Consequently, a solution to the heat equation with surface radiation is

$$H(x,t) = \frac{b}{(4\pi\theta)^{1/2}} x t^{-3/2} \exp\left(-\frac{x^2}{4\theta t} - \lambda t\right). \tag{5}$$

For a fixed depth x, Equation (5) can be written as a 3 parameter function of time, namely

$$h(t|\beta) = \beta_1 t^{-3/2} \exp\left(-\frac{\beta_2}{t} - \beta_3 t\right) \quad \text{with } \beta_1, \beta_2, \beta_3 \geq 0. \tag{6}$$

Estimates of the parameters $(\beta_1, \beta_2, \beta_3)$ were obtained for each profile separately using a nonlinear least-square routine. The independent error structure assumed in nonlinear least-square routines is often not valid for functional data. Adequacy of the model, including the independent error assumption, was studied by producing residuals (observed-predicted) and autocorrelation functions of residuals.

The left hand column of Fig. 4 contains graphs of the observed and fitted profiles for 6 records at 10 cm depths. The fits were obtained by estimating the parameters $(\beta_1, \beta_2, \beta_3)$ using the nonlinear least-square (nls) function within the S-PLUS statistical package (SPLUS 4, 1997). A systematic difference between the observed (solid) and predicted (dashed) curves is noted in many of the records. The temperatures in many of the observed profiles starting around 60 h were systematically greater than predicted. In other words, temperatures in the soil appear to be decreasing slower than expected under the above model.

There are many processes by which heat transfer occurs in soil. Two of the processes included in the model above are conduction and radiation. The apparent rates of conduction and radiation (assumed fixed in the models above) are very likely changing over the course of the fire. For example, a layer of ash deposited on the soil surface in the course of a fire will have the effect of reducing the apparent emissivity (rate of radiation) of the soil surface (Pafford *et al.*, 1985). In wet soils, the thermal conductivity and diffusivity of the soil ''will change with time due to drying of the soil adjacent to the heat source'' (Moench and Evans, 1970).

A modified model that allows thermal parameters to change over time is obtained by adding a second degree term $(\beta_4 t^2)$ to the exponent of the exponential in Equation (6), and by allowing β_3 to be negative. The fits with the 4-parameter modified model showed a substantial improvement when compared to the fits with the 3-parameter model (Fig. 4).

A further study of the goodness of fit of the 4-parameter model was done by producing autocorrelation functions of residuals. Fig. 5 is a graph of the autocorrelation function (Shumway, 1988) for the first differences of the residuals for profile R4 produced using the

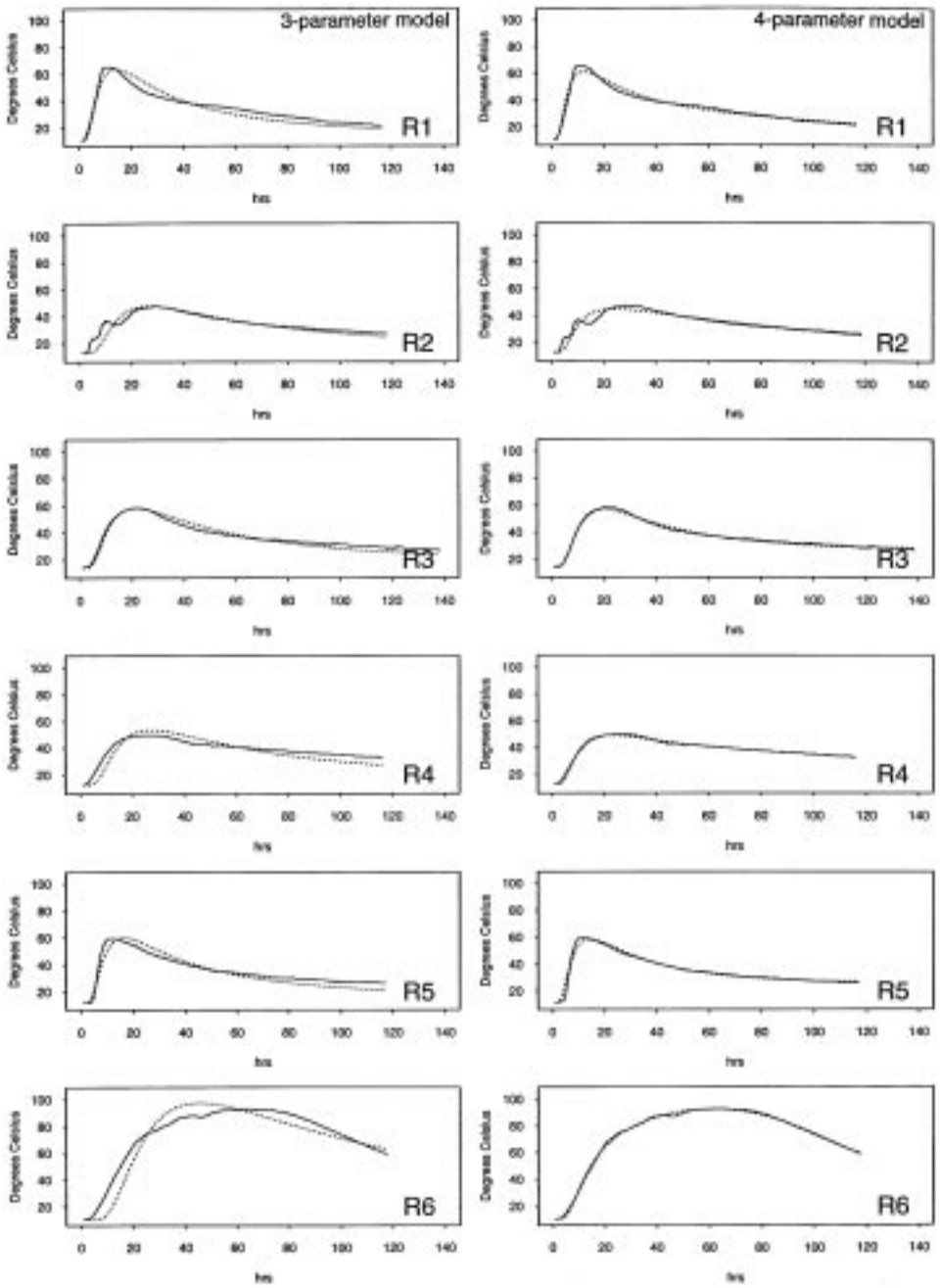

Figure 4. Left panels are observed profiles (solid curves) of six records at 10 cm depth compared with fitted profiles (dashed lines) produced by a nonlinear fit of the three parameter model. Right panels are observed profiles (solid curves) compared with fitted profiles (dashed lines) produced by fitting the four parameter model.

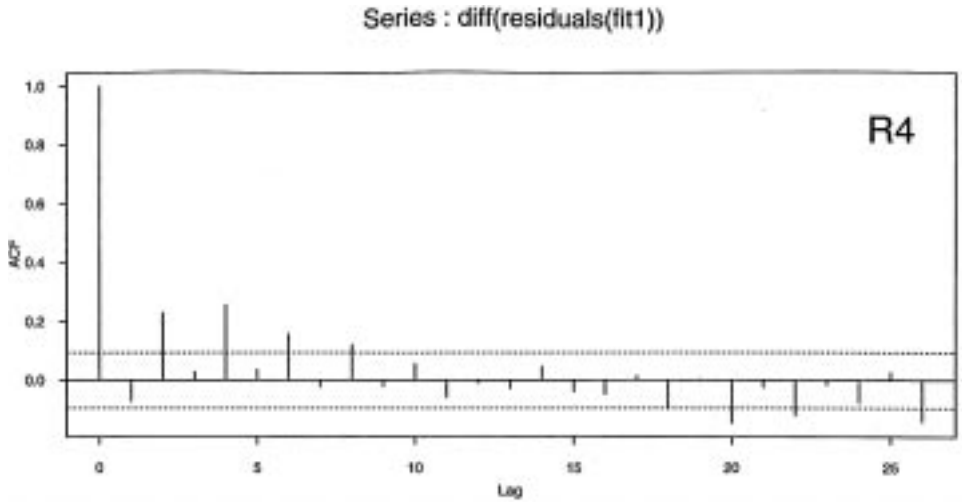

Figure 5. Estimated autocorrelation function of first differences of the residual series for record four.

acf function in SPLUS. Specifically, if $y_{t_i}, i = 1, \ldots, n$ are the observed temperatures in a given profile at times t_i and $h(t_i|\hat{\beta})$ are the predicted temperatures, then the sample autocorrelation function, $\rho(k)$, at lag k for the difference of the residuals is given by $\rho(k) = \frac{\gamma(k)}{\gamma(0)}$ where

$$\gamma(k) = \frac{1}{n}\sum_{i=1}^{n-k}(x_t - \bar{x})(x_{t+k} - \bar{x}); \quad x_t = r_t - r_{t-1}; \quad \bar{x} = \frac{1}{n}\sum_{t=1}^{n} x_t; \quad r_t = y_t - h(t|\hat{\beta}).$$

The autocorrelation function summarizes the dependence of observations in the same record at different lags (intervals of time). The dotted horizontal lines in the autocorrelation plot in Fig. 5 are approximate 95% confidence limits for pure noise series. The autocorrelation of a pure noise series is equal to 1 for $t = 0$, and zero otherwise. In most of the records, the first difference series of the residuals appears similar to pure noise, indicating an autoregressive model, with the error structure $\varepsilon_t = \varepsilon_{t-1} + u_t$ and with u_t a Gaussian white noise series. In cases where an autoregressive model of order one was not adequate, an autoregressive model of order 2 seemed to be sufficient. Consequently, a useful stochastic model for individual temperature profiles is

$$h(t|\beta) = t^{-3/2}\exp\left(\beta_0 - \frac{\beta_2}{t} + \beta_3 t + \beta_4 t^2\right) + \varepsilon_t \qquad \beta_2 \geq 0 \tag{7}$$

with $\varepsilon_t = \rho_1\varepsilon_{t-1} + \rho_2\varepsilon_{t-2} + u_t$; and u_t is Gaussian white noise.

We used the model in (7) to obtain estimates of the parameters and estimates of the standard errors. The fitting was done using the Cochran-Orcutt two-stage procedure (Shumway 1988). In the first stage, estimates for ρ were obtianed by fitting an autoregressive model to the residuals, $r_t = y_t - h(t|\hat{\beta})$, from the ordinary least-square fit (we used the linear mixed effect (lme) procedure in SPLUS for this stage). In the second

stage, the parameters $\{\beta_0, \beta_2, \beta_3, \beta_4\}$ were reestimated in a nonlinear regression model of the form

$$z_t = y_t - \hat{\rho}_1 y_{t-1} - \hat{\rho}_2 y_{t-2} = h(t|\beta) - \hat{\rho}_1 h(t-1|\beta) - \hat{\rho}_2 h(t-2|\beta) + u_t \qquad (8)$$

where u_t are independent Gaussian errors and $h(t|\beta)$ given by Equation (7). Under the Gaussian error model the two-stage procedure is expected to converge to the maximum likelihood estimates (Shumway, 1988).

In almost all cases studied, estimates of ρ_1 were close to one (>0.97) and estimate of ρ_2 were close to zero (<0.05). This result is not surprising considering that temperatures were recorded every 15 min. Estimated values of the β parameters (and standard error estimates) for a typical profile at 10 cm depth (R4 in Fig. 4) were,

$$\hat{\beta}_0 = 9.222 \pm 0.066, \quad \hat{\beta}_2 = 3.0 \pm 0.025, \quad \hat{\beta}_3 = 0.027 \pm 0.002,$$

$$\hat{\beta}_4 = (-1.1 \pm 0.139) \times 10^{-4}.$$

In the next section we study the effects of site characteristics on maximum temperatures estimated from the fitted curves, and estimate the risks of temperatures exceeding critical levels. Maximum temperatures calculated from fitted curves use all of the data points in a record to estimate maxima. Consequently, they are less likely to be affected by recording errors or local fluctuations than are observed maxima. A functional form of the tempera ture profile is also useful for calculating maxima in records with irregularly spaced observa tions and for calculating other features of the profile, such as, the number of hours tempera tures stay above a given level, or the area under the curve above a critical threshold.

4. Predicting maximum temperatures and risks of exceeding critical temperatures

Effects of the observed site characteristics on estimated maximum temperatures were best described by the random effects model

$$\begin{aligned} y_{ijk} = \log(T_{ijk}) = {} & 4.34 - 0.0230 \times \text{depth}_{ijk} + 0.00226 \times \text{fuel}_{ij} - 0.0240 \times \text{moist}_{ij} + \varepsilon_{ij} + \varepsilon_{ijk} \\ & (0.16)\ (0.0014) \qquad (0.00068) \qquad (0.0097) \end{aligned} \qquad (9)$$

where T_{ijk} is the estimated maximum temperature in fire i, location j, depth k; depth_{ijk} is the depth (cm) of the kth thermocoupler at location j fire i; fuel_{ij} is the fuel loading (Mg/hectare) at location j, fire i; moist_{ij} is the moisture level (%) at 5–10 cm from soil surface at location j, fire i; ε_{ij} is the random effect of the jth location within the ith fire; ε_{ijk} is the residual random error.

The numbers in parentheses under the coefficient estimates in Equation (9) are the standard error estimates for the respective coefficients. Two other site characteristics, surface moisture and tree type (Sequoia or Sugar Pine), had no significant effects (likelihood ratio test P-value $= 0.17$) on maximum temperature. The random terms ε_{ij}, ε_{ijk}, were assumed to be independent Gaussian variates with variances τ^2 and σ^2, respectively. Random location effects ε_{ij}, were included in the model to account for correlations between records from the same location within a fire. Correlations between

records from different locations within the same fire were not included in the final model because the between fire variation was found to be negligible (estimate of standard error $< 10^{-5}$) when compared with the variation between locations within the same fire ($\hat{\nu} = 0.19$) or the record-to-record variation ($\hat{\sigma} = 0.16$). The variance of the residual error (ε_{ijk}) could also be made proportional to the variance of the estimated maximum temperature by using weighted nonlinear regression.

Goodness of fit of the model in (9) was checked by producing diagnostic plots of partial residuals against the independent variables, depth, fuel, and moisture (Fig. 6). Partial

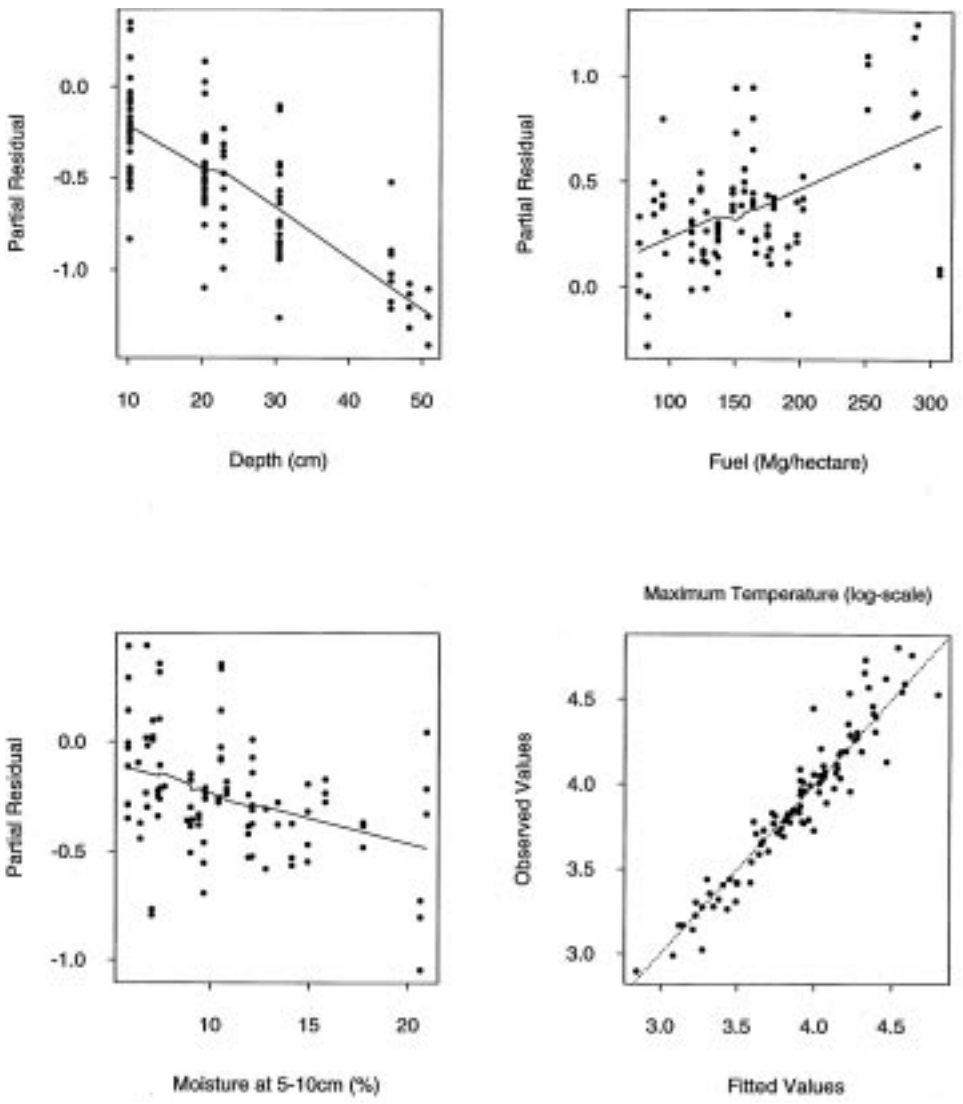

Figure 6. Diagnostic plots of partial residuals and fitted values from the random effects model with logarithm of maximum temperature as the dependent variable. The smoothed partial residuals were produced by a variable span super smoother.

residuals are defined by $u = y - (\hat{y} - \hat{\beta}x)$, where x is one of the independent variables (McCullagh and Nelder, 1989). Partial residual plots tend to be more informative than scatterplots of dependent against independent variables because they show the relationships between y and each independent variables after removing estimated effects of all other independent variable. The smooth curves through the points, produced by a nonparametric smoother (supsmu procedure in SPLUS, Cleveland and Devlin, 1988; Friedman, 1984); seem to justify the linear relationships used in (9). The plot of observed versus fitted values (last panel in Fig. 6) is another indication that the linear mixed effect model in (9) does a reasonable job of explaining the maximum temperature values.

The estimated regression relationship between maximum temperature and measured site characteristics can be use to calculate risk probabilities that temperatures in a future fire will exceed a given critical level T_C. With the errors ε_{ij} and ε_{ijk} assumed to be independent-Gaussian and the between fire error ε_i assumed to be negligible, the risk probability function is given by $1 - \Phi(\eta)$, where an estimate of η for a given fuel level m and moisture level l is given by

$$\hat{\eta}_{lm} = (\log T_C - \log \hat{T}_{lm})/(\hat{\nu}^2 + \hat{\sigma}^2)$$

where $\log \hat{T}$ is given by Equation (8), Φ the Gaussian distribution, and $\hat{\nu}$ and $\hat{\sigma}$ as above. Estimates of the standard errors of $\hat{\eta}$ are obtained using the delta method (Bishop *et al.*, 1975). Finally, 95% intervals for the probabilities of interest are calculated by

$$1 - \Phi(\hat{\eta} + 1.96\hat{\sigma}_\eta) < 1 - \Phi(\eta) < 1 - \Phi(\hat{\eta} - 1.96\hat{\sigma}_\eta).$$

Fig. 7 provides estimates for probabilities of temperatures in a future fire exceeding 60°C if the soil moisture level at 5–10 cm is 7% or 15% and for fuel levels between 78 to 303 Mg/hectare (range of observed fuel levels in data). According to these estimates, the risk of exceeding 60°C at 10 cm depth when the soil moisture level is 7% is $>50\%$ for all observed fuel levels. This risk decreases when the soil moisture level is 15%. Comparing point estimates, the estimated risk of exceeding 60°C at a depth of 20 cm is about 20% lower than the risk closer to the the surface (10 cm). However, when the standard error estimates (the vertical bars) are taken into account, the risks at the two depths are not different; the standard error estimates are very wide. These estimates might improve if the number of records analyzed is increased. However, much of the variation may be inavoidable because of natural variation in unobserved site characteristics among fire locations.

5. Conclusions

In this article we presented methods for analyzing soil temperature profile data recorded during prescribed forest fires. We found the use of robust/resistant methods for calculating summary statistics of functional data useful for producing graphs of mean temporal temperature profiles. We were able to make the following conclusions from the summary graphs: (1) There were significant drops in mean temperatures for every 10 cm drop in depth (for depth of 10–46 cm below soil level) during the first day after the start of the fire; (2) by the end of the second day there cease to be significant differences in mean temperatures at the four observed depths; and (3) five days after the start of the fire, mean

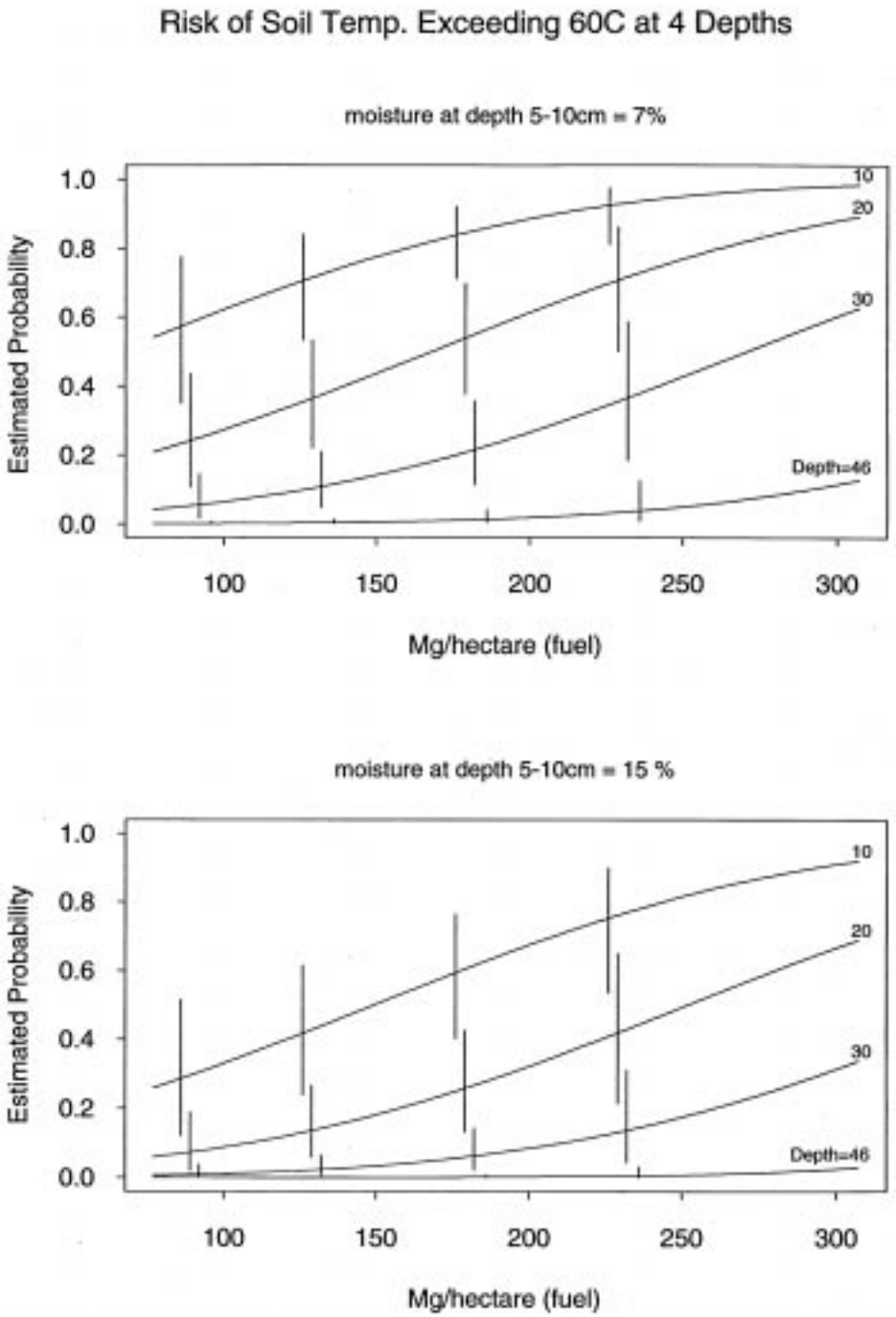

Figure 7. Contour plots of estimated probabilities associated with risk of temperatures in a future fire exceeding the critical level of 60°C. Each contour represents estimates of the probabilities for a given depth; 95% pointwise prediction intervals (vertical bars) are given for 4 points on each contour.

temperatures at all 4 depths were 11°C higher than ambient soil temperatures before the fire.

A stochastic model that seemed to best fit the temperature profile data was an autoregressive model of order one or two with the expected value given by a four parameter nonlinear curve. The expected curve was based on the so called ''derived source solution'' of the partial differential equation for heat conduction first proposed by Fourier (1878) to calculate the temperature of the ground at a given depth due to the sun's heating. The four parameter model was a modification of the derived source solution that accommodates surface radiation and allows the apparent rates of conduction and/or radiation to change over time. One expects thermal conductivity of the soil and the surface radiation to change in the course of a fire due to drying soil and due to layers of ash depositing on the soil.

Values of interest to forest managers are estimates of probabilities identifying specific risks associated with prescribed burns. Here we demonstrated the use of a sample of temperature profiles from different fires to estimate probabilities associated with a particular risk, that of temperatures exceeding the critical level of 60°C at which point protoplasm coagulates and tissues die. The contour plots we produced for this risk can be used to predict the probability of temperatures in a future fire, at a site similar to the ones in this study and with a given fuel loading and moisture level, exceeding 60°C. According to our estimates, the probability of temperatures at 10 cm below the soil level exceeding 60°C is greater than 50% for all fuel levels greater than 90 Mg/hectare when the moisture level at the 5–10 cm depth was low (7%). The same probability estimates were lower, although not significantly lower, when the moisture level increased to 15%. The approximate 95% pointwise confidence intervals for probabilities in a future fire were very broad, especially for fuel values greater than 200 Mg/hectare; the number of records with fuel values greater than 200 Mg/hectare were small (see Fig. 6). Probabilities of other risks of interest can also be estimated using random effects models similar to the one proposed in this paper.

Acknowledgments

We wish to thank Gloria Bruke for help with the collection and storage of the prescribed fire data. We also would like to thank the reviewers for their helpful suggestions which improved the presentation and content of the manuscript.

References

Bishop, Y.M.M., Fienberg, S.E., and Holland, P.W. (1975) *Discrete Multivariate Analysis: Theory and Practice*, MIT Press, Cambridge, MA, p. 486.

Brillinger, D.R. (1981) Söme aspects of the analysis of evoked response experiments. In *Statistics and Related Topics* (M. Csörgö, D.A. Dawson, J.N.K. Rao and A.K. Md. E. Saleh, eds.), North-Holland, Amsterdam, pp. 155–68.

Campbell, G.S., Jungbauer, J.D., Bristow, JR. K.L., and Hungerford, R.D. (1995) Soil temperature and water content beneath a surface fire. *Soil Science*, **159**, 363–74.

Christiansen, K. (1964) Bionomics of Collembola. *Annual Rev. Entom.*, **9**, 147–78.

Cleveland, W.S. and Devlin, S.J. (1988) Locally-weighted regression: An approach to regression analysis by local fitting. *Journal of the American Statistical Association*, **83**, 596–610.

Covington, W.W. and Sackett, S.S. (1990) Fire effects on ponderosa pine soils and their management implications. In *Proceedings of the Symposium on Effects of Fire Management of southwestern Natural Resources* (J.S. Krammes, ed.). General technical report RM-191, U.S.D.A., Forest Service, Rocky Mountain Forest and Range Experiment Station, Fort Collins, CO, pp. 105–11.

El-Doma, M.O., Locke, B., Primack, D., Gould, K., and Knapp, R. (1984) Modelling heat and moisture transfer for prescribed fire in Southern California. *The Mathematics Clinic*, Interim Report to Forest Service, U.S. Department of Agriculture, 46 pp.

Efron, B. (1982) *The Jackknife, the Bootstrap and other Resampling Plans*, Society for Industrial and Applied Mathematics, Philadelphia, Pennsylvania, 92 pp.

Folledo, M. (1983) *Robust/resistant methods in the estimation of the evoked response curve*, Ph.D. thesis, University of California, Berkeley.

Fourier, J. (1878) *Analytic Theory of Heat*, Cambridge University Press, Cambridge.

Friedman, J.H. (1984) *A variable span smoother*, Technichal Report 5, Laboratory of Computational Statistics, Department of Statistics, Stanford University, Stanford, CA.

Haase, S.M. and Sackett, S.S. (1998) Effects of prescribed fire in gaint sequoia-mixed conifer stands in Sequoia and Kings Canyon National Parks. In *Proceedings of the tall timbers Fire Ecology Conference* (L.A. Brennan and T.L. Pruden, eds.), No. 20. Tall Timbers Research Station, Tallahassee, FL.

Hungerford, R.D., Harrington, M.G., Frandsen, W.H., Ryan, K.C., and Niehoff, G.J. (1991) Influences of fire on factors that affect site productivity. In *Proceedings of the Management and Productivity of Western-Montane forest soils* (A.E. Harvey and L.F. Neuenschwander, eds.), U.S.D.A., Forest Service, Intermountain Research Station General Technical Report INT-280.

Kayll, A.J. (1963) *Heat tolerance of Scots pine seedling cambium using tetrazolium chloride to test viability*, Publication No. 1006, Canada Department of Forestry, Forest Resources Branch.

Lorenz, R.M. (1939) *High temperature tolerance of forest trees*, Technical Bulletin 141, Agricultural Experiment Station, University of Minnesota.

Moench, A.F. and Evan, D.D. (1970) Thermal conductivity and diffusivity of soil using a cylindrical heat source, *Soil Science Society of America Proceeding*, **34**, 377–81.

McCullagh, P. and Nelder, J.A. (1989) *Generalized Linear Models*, 2nd edition, Chapman and Hall, London.

Nelson, R.M. (1952) *Observations of heat tolerance of southern pines*, Paper 14, U.S. Department of Agriculture, Forest Service, Southern Forest Experiment Station, Ashville, NC.

Pafford, D., Dhir, V.K., Anderson, E.B., and Cohen, J. (1985) *A model for ground surface heating during a prescribed burn*, Eighth Conference on Fire and Forest Meteorology, Society of American Foresters, pp. 24–32.

Piaggio, H.T.H. (1937) *Differential Equations*, G. Bell and Sons, London.

Ramsay, J.O. and Silverman, B.W. (1997) *Functional Data Analysis*, Springer-Verlag, New York, 310 pp.

Sackett, S.S. and Haase, S.M. (1992) *Measuring soil and tree temperatures during prescribed fires with thermocouple probes*, General Technical Report PSW-131. U.S.D.A., Forest Service, Pacific Southwest Research Station, Albany, CA.

Shumway, R.H. (1988) *Applied Statistical Time Series Analysis*, Prentice-Hall, New Jersey, p. 192.

S-PLUS 4 Guide to Statistics, Data Analysis Products Division, MathSoft, Seattle.

Widder, D.V. (1975) *The Heat Equation*, Academic Press, New York, 267 pp.

Biographical sketches

Haiganoush K. Preisler is a Mathematical Statistician at USDA Forest Service, Pacific Southwest Research Station. She received her Ph.D. in statistics from University of California, Berkeley in 1977 and her MS from American University of Beirut, Lebanon in 1972. Her current work focuses on applications of stochastic models to studies of effects of natural and human disturbances on the forest ecosystem.

Sally M. Haase is a Research Forester (fire) for USDA Forest Service, Pacific Southwest Research Station, located at the Forest Fire Laboratory in Riverside, CA. She has over twenty years experience in prescribed fire research in the southwestern ponderosa pine ecosystem and has expanded into California conifer ecosystem.

Stephen S. Sackett is a Research Forester (fire) for the USDA Forest Service, Pacific Southwest Research Station, located at the Forest Fire Laboratory in Riverside, CA. He has over thirty-four years experience in prescribed fire research spanning from southeastern to southwestern United States. He has concentrated on prescribed fire effects above and below ground on areas that have had repeated burns.